

# Development of semiconductor imaging detectors for a Si/CdTe Compton camera

Shin Watanabe<sup>a,\*</sup>, Shin'ichiro Takeda<sup>a,b</sup>, Shin-nosuke Ishikawa<sup>a,b</sup>, Hirokazu Odaka<sup>a,b</sup>,  
Masayoshi Ushio<sup>a,b</sup>, Takaaki Tanaka<sup>a,b</sup>, Kazuhiro Nakazawa<sup>a</sup>, Tadayuki Takahashi<sup>a,b</sup>,  
Hiroyasu Tajima<sup>c</sup>, Yasushi Fukazawa<sup>d</sup>, Yoshikatsu Kuroda<sup>e</sup>, Mitsunobu Onishi<sup>e</sup>

<sup>a</sup>*Institute of Space and Astronautical Science, Japan Aerospace Exploration Agency, 3-1-1 Yoshinodai, Sagami-hara, Kanagawa 229-8510, Japan*

<sup>b</sup>*Department of Physics, The University of Tokyo, Bunkyo, Tokyo 113-0033, Japan*

<sup>c</sup>*Stanford Linear Accelerator Center, Menlo Park, CA, USA*

<sup>d</sup>*Department of Physics, Hiroshima University, Higashi Hiroshima, Hiroshima, Japan*

<sup>e</sup>*Nagoya Guidance and Propulsion System Works, Mitsubishi Heavy Industries, Ltd., Komaki, Aichi 485-8561, Japan*

## Abstract

Si and CdTe semiconductor imaging detectors have been developed for use in a Si/CdTe Compton camera. Based on a previous study using the first prototype of a Si/CdTe Compton camera, new detector modules have been designed to upgrade the performance of the Compton camera. As the scatter detector of the Compton camera, a stack of double-sided Si strip detector (DSSD) modules, which has four layers with a stack pitch of 2 mm, was constructed. By using the stack DSSDs, an energy resolution of 1.5 keV (FWHM) was achieved. For the absorber detector, the CdTe pixel detector modules were built and a CdTe pixel detector stack using these modules was also constructed. A high energy resolution ( $\Delta E/E \sim 1\%$ ) was achieved. The improvement of the detection efficiency by stacking the modules has been confirmed by tests of the CdTe stack. Additionally, a large area CdTe imager is introduced as one application of the CdTe pixel detector module.

## 1. Introduction

The Compton camera is the most promising approach for gamma-ray imaging and spectroscopy in the range of several tens keV to several MeV. For Compton cameras, both good energy resolution and good position resolution are very important to achieve a Compton reconstruction that has high levels of accuracy. We propose a new concept of the Si/CdTe semiconductor Compton cameras based on our developments of Si and CdTe semiconductor imaging detectors [1,2].

The basic concept of the Si/CdTe Compton camera is shown in Fig. 1. Double-sided Si strip detectors (DSSDs)

are used as scatterers and CdTe pixel detectors are used as absorbers. In order to increase the efficiency of Compton scattering, the DSSDs are tightly stacked in many layers. The CdTe pixel detectors are arranged around the DSSD stack to detect scattered gamma-rays with high efficiency.

When a gamma-ray photon is scattered in one DSSD and absorbed in one CdTe pixel detector, the incident energy of the gamma-ray and the scattering angle can be determined as

$$E_{\text{in}} = E_1 + E_2 \quad (1)$$

$$\cos \theta = 1 - \frac{m_e c^2}{E_2} + \frac{m_e c^2}{E_1 + E_2} \quad (2)$$

where  $E_{\text{in}}$  is the incident energy,  $E_1$  is the energy of the recoil electron detected in the DSSD,  $E_2$  is the energy of the

\*Corresponding author.

E-mail address: watanabe@astro.isas.jaxa.jp (S. Watanabe).

scattered photon absorbed by the CdTe and  $\theta$  is the scattering angle. If one measures the Compton scattering point, recoil electron energy, and scattered gamma-ray energy and position relative to the Compton scattering point, then the energy of the incident gamma-ray is determined, and the direction of the incident gamma-ray lies somewhere on a cone defined by these measurements.

The combination of Si and CdTe is suitable for gamma-rays that range from several tens of keV to a few MeV. The photo-absorption cross-section of Si is small, and the Compton cross-section becomes relatively large because of the small atomic number of Si ( $Z = 14$ ). Additionally, Si works better than other materials with larger atomic numbers in terms of the “Doppler broadening” effect [3].

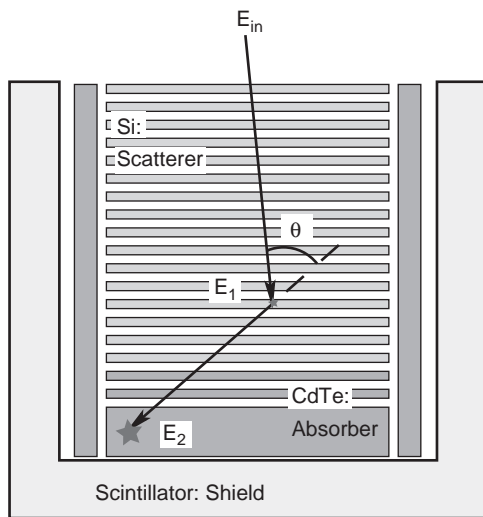


Fig. 1. Schematic picture of our Si/CdTe semiconductor Compton camera.

On the other hand, CdTe has high photo-absorption efficiency for gamma-rays in this energy region, due to their high atomic numbers of 48 and 52.

## 2. The results from the first prototype of the Si/CdTe Compton camera

We constructed a prototype of the Si/CdTe Compton camera in order to demonstrate the concept described above [4,5]. The prototype consisted of six layers of DSSDs and three CdTe pixel detectors. The DSSD has an area of  $2.56\text{ cm} \times 2.56\text{ cm}$  and a thickness of  $300\text{ }\mu\text{m}$ . The strip pitch of the DSSD is  $400\text{ }\mu\text{m}$  and each side has 64 strips. The CdTe pixel detector is based on the Schottky CdTe diode device, utilizing indium as the anode and platinum as the cathode [6,7]. The CdTe crystal is manufactured by ACRORAD in Japan using the Traveling Heater Method. The detector has dimensions of  $18.55\text{ mm} \times 18.55\text{ mm}$  and a thickness of  $500\text{ }\mu\text{m}$ . The indium side is used as a common electrode. The platinum side is divided into  $8 \times 8$  pixel sections surrounded by a  $1\text{ mm}$  wide guard ring. The pixel size is  $2\text{ mm} \times 2\text{ mm}$ , and the gap between the pixels is  $50\text{ }\mu\text{m}$ . Each pixel is connected to a fanout board by using In/Au stud bump bonding technology [8]. The signals from the DSSDs and CdTe pixel detectors are processed by low noise analog ASICs, VA32TAs.

By irradiating the prototype with gamma-rays from radio isotopes ( $^{133}\text{Ba}$ ,  $^{57}\text{Co}$ ,  $^{22}\text{Na}$  and  $^{137}\text{Cs}$ ), we have successfully obtained Compton reconstructed images and spectra from 80 to 662 keV. Fig. 2 shows Compton reconstructed images of  $^{133}\text{Ba}$  and  $^{22}\text{Na}$  sources obtained with the Compton camera. These images are drawn using conventional Compton reconstruction. First, we select “two-hit events”; that is, one hit to the DSSD and one

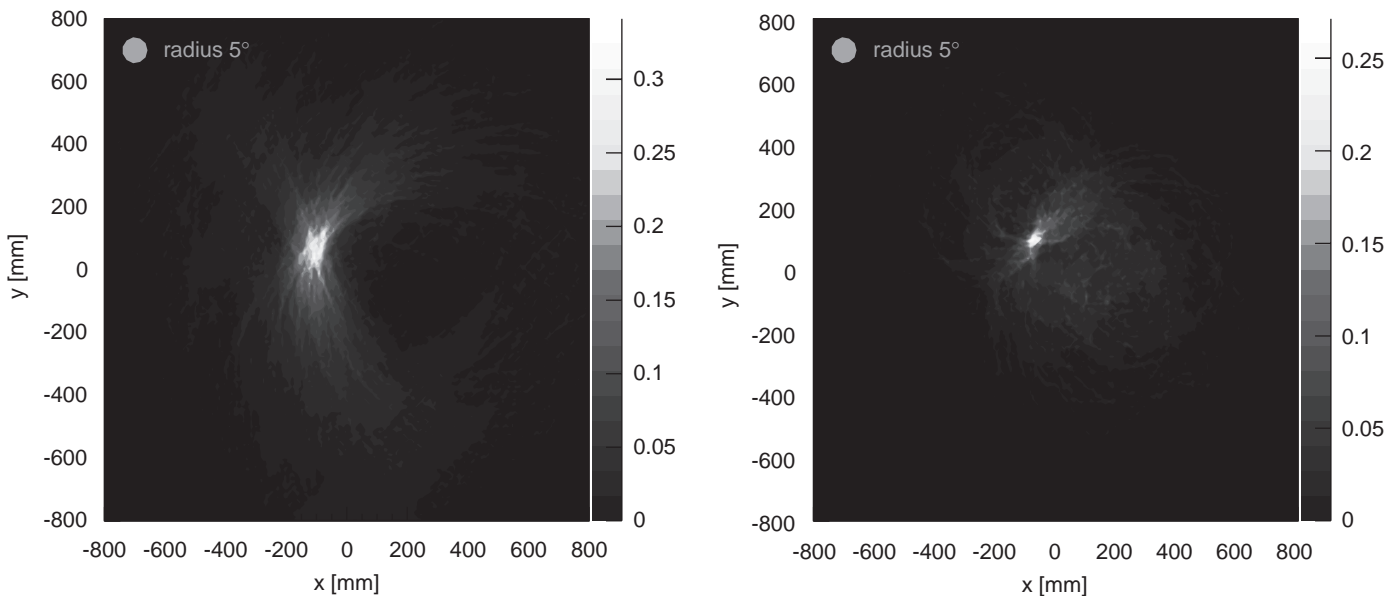


Fig. 2. Compton reconstructed images of 80 keV gamma-rays from  $^{133}\text{Ba}$  (left) and 511 keV gamma-rays from  $^{22}\text{Na}$  (right). Circles with a radius of  $5^\circ$  are drawn together with the images.

hit to the CdTe. The scatter angle is obtained for each two-hit event. From the scatter angle and the two-hit positions, a Compton cone is drawn on the sky event by event. We then project the cone onto the plane, and obtain the final image.

Due to the good energy resolution of both the DSSDs and the CdTe pixel detectors, good angular resolution was obtained. The achieved angular resolution almost reaches the theoretical limit due to Doppler broadening. Additionally, an important point to note is that the Compton reconstruction for low energy gamma-rays such as 80 keV is achieved. When 80 keV gamma-rays are scattered, the energy of the Compton recoiled electron is only about 10 keV. The achieved energy threshold level is 6 keV for our DSSDs. This is what enabled us to obtain the Compton image for such low energy gamma-rays.

We have established a working model of the Si/CdTe semiconductor Compton camera concept with this prototype. The prototype experiment demonstrates that it is possible to build a Si/CdTe Compton camera that reaches the theoretical limit of angular resolution as a result of Doppler broadening. In response to the prototype results, we have set our goal: Si/CdTe semiconductor Compton cameras with a 1% energy resolution ( $\Delta E(\text{FWHM})/E$ ), the Doppler-limited angular resolution and a 10% detection efficiency. In the following sections, we report our developments of DSSDs and CdTe pixel detectors for the next version of the Compton camera.

### 3. Development of a new DSSD stack

First of all, in order to improve the efficiency of Compton scattering, a tight stack of DSSDs is necessary. We therefore designed and constructed new DSSD modules to create a compact DSSD stack. Fig. 3 shows pictures of the DSSD module. The size of the DSSD is  $2.56\text{ cm} \times 2.56\text{ cm}$  with a thickness of  $300\text{ }\mu\text{m}$ . The strip pitch is  $400\text{ }\mu\text{m}$ . Each side has 64 strips and the signals from the strips are processed by new analog ASICs, VA64TAs, which were developed by this research team in conjunction with IDEAS. The VA64TA features low noise performance and low power consumption [5].

The stack pitch of 2 mm is available by using the DSSD modules. For 10% Compton efficiency, 40 layers of  $300\text{ }\mu\text{m}$  thick DSSDs or 24 layers of  $500\text{ }\mu\text{m}$  thick DSSDs are required [9,10]. It is essential to reduce the gap between the DSSD layers and to stack them tightly. If DSSDs are stacked loosely, the DSSD stack becomes too tall. In this case, too many CdTe detectors are needed to prevent the gamma-ray photons scattered in the DSSDs from escaping.

It is also important to reduce material around the DSSDs for effective detections of low energy ( $\sim 100\text{ keV}$ ) gamma-ray in the Compton camera. The gamma-ray photons scattered in DSSDs must reach an absorber detector directly without being scattered or absorbed. Therefore, we have used kapton plastic as the DSSD jig

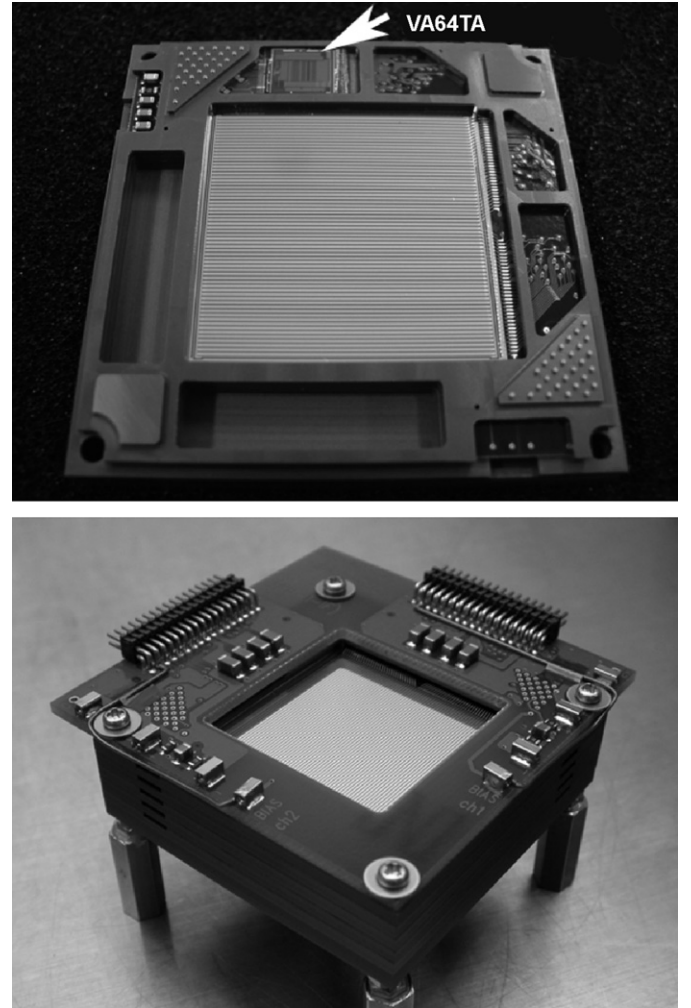


Fig. 3. The new DSSD module and the new DSSD stack. The size of the DSSD is  $2.56\text{ cm} \times 2.56\text{ cm}$ . The  $0.3\text{ mm}$  thick DSSDs are stacked in four layers. The pitch between the layers is  $2\text{ mm}$ .

material instead of the  $\text{Al}_2\text{O}_3$  ceramic used in previous modules.

For the first step, we have stacked the DSSD modules in four layers and have tested the DSSD stack in photo-absorption mode by applying a bias voltage of  $100\text{ V}$  between the P-side and the N-side. Fig. 4 shows gamma-ray spectra obtained with P-side strips. The average energy resolution from all P-side strips was  $1.5\text{ keV}$  (FWHM) at  $59.54\text{ keV}$  with an operating temperature of  $-10^\circ\text{C}$ . More details about the DSSD modules' properties are described in Takeda et al. [11].

### 4. CdTe Pixel detector module

In the Si/CdTe Compton camera, CdTe pixel detectors have to cover the DSSD stack with a large solid angle in order to absorb as many gamma-rays scattered in the DSSDs as possible. We designed a CdTe pixel detector module and constructed a number of these modules.

Fig. 5 shows the newly developed CdTe pixel module. The CdTe crystal is manufactured by ACRORAD in Japan

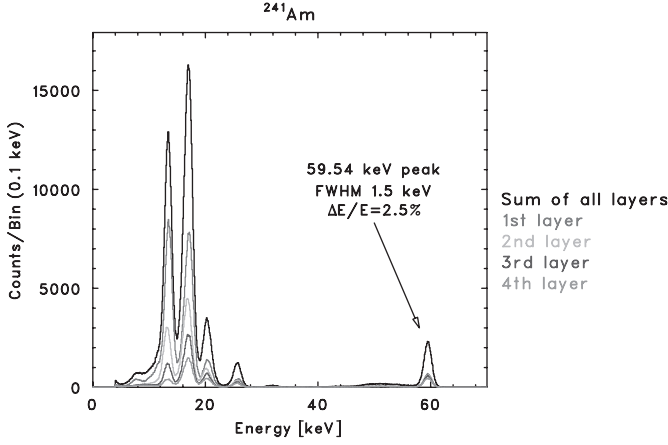


Fig. 4.  $^{241}\text{Am}$  spectra obtained with the DSSD stack. The grays show spectra from the first layer, the second layer, the third layer and the fourth layer, respectively. The black spectrum shows the sum of all layers. The achieved energy resolution is 1.5 keV (FWHM) at 59.54 keV. The operating temperature is  $-10^\circ\text{C}$ .

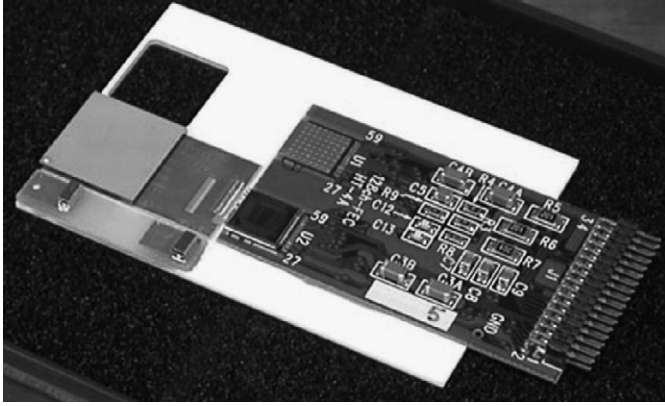


Fig. 5. The newly developed CdTe pixel detector module.

using the Traveling Heater Method. The size of the CdTe device is  $13.35\text{ mm} \times 13.35\text{ mm}$  and the thickness is 0.5 mm. This is a Schottky CdTe diode device, utilizing indium as the anode and platinum as the cathode [6,7,12,13]. The indium side is used as a common electrode, and the platinum side is divided into  $8 \times 8 = 64$  pixels. The pixel size is  $1.35\text{ mm} \times 1.35\text{ mm}$ , and the gap between the pixel electrodes is  $50\text{ }\mu\text{m}$ . Around the pixels, a guard ring electrode with a width of 1 mm is attached. This is attached so as to reduce leakage current, as most of the leakage current occurs through the device perimeter [14]. Additionally, a thin layer of gold is evaporated on the Pt side for the purpose of the ensuring good bump bonding connectivity.

In order to connect the pixels to the one-dimensional ASIC, a fanout board was designed. The substrate of the fanout board is made from a 96%  $\text{Al}_2\text{O}_3$  ceramic with a thickness of  $300\text{ }\mu\text{m}$ . The fanout board consists of bump pads, through-holes and patterns that route the signal from bump pads on both surfaces of the ceramic substrate.

Each pixel is connected to the bump pads on the fanout board by In/Au stud bump bonding technology, developed specifically for CdTe detectors [8]. A needle-shaped stud consisting of two stages of gold studs is fixed to the bump pad of the fanout board. The studs are made with a gold wire, and a thin layer of indium is printed on the top of the stud. There are 92 studs, including 64 for the pixels and 28 for the guard ring. The CdTe device and the fanout board are then pressed under controlled temperature conditions. In the previous design of the CdTe pixel detector, epoxy resin was used to fill in the space between the CdTe device and the fanout board. However, we found that epoxy resin degraded electrical resistance properties. Therefore, in this version, no epoxy resin was used. The mechanical strength of the module is still maintained, even without the use of epoxy resin.

Before wire bonding from the fanout board to the ASIC, we measured the leakage current. In our previous study, we found that the leakage current measurements of the detectors assist in the selection of good detectors [15]. The setup of the leakage current measurement is shown in Fig. 6. The sum leakage current of all 64 pixels and that of the guard ring were simultaneously measured separately. By bringing a probe into contact with the through hole on the ceramic fanout board, the pixel electrode side can be accessed without damaging the electrodes. We took the  $I$ - $V$  curve up to 700 V and the time variation of the leakage current under a bias voltage of 700 V at a temperature of  $20^\circ\text{C}$ . We then performed the selections to build up the pixel modules. The selection criterion is that the leakage current under the bias voltage of 700 V must be stable. This is, any variance must remain within a 10% variation range for a period of two hours.

We measured the leakage currents of 106 bump bonded CdTe devices and selected 74 devices from these. The distribution of the leakage currents for the pixels under a bias voltage of 700 V in a temperature of  $20^\circ\text{C}$  approximated the Landau distribution. The most probable value was 1.2 nA and the sigma was 0.19 nA. Each selected device was wire bonded to a VA64TA. CdTe pixel modules were then created from the selected devices.

We tested the pixel modules by irradiating them with gamma-rays from radio isotopes. Fig. 7 shows  $^{241}\text{Am}$  and  $^{57}\text{Co}$  spectra obtained from one of the CdTe pixel detector

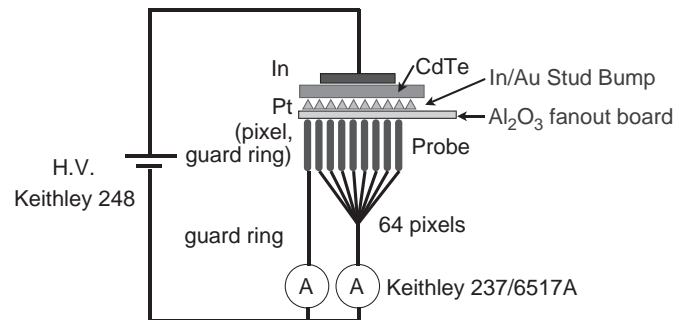


Fig. 6. The setup of the leakage current measurement.



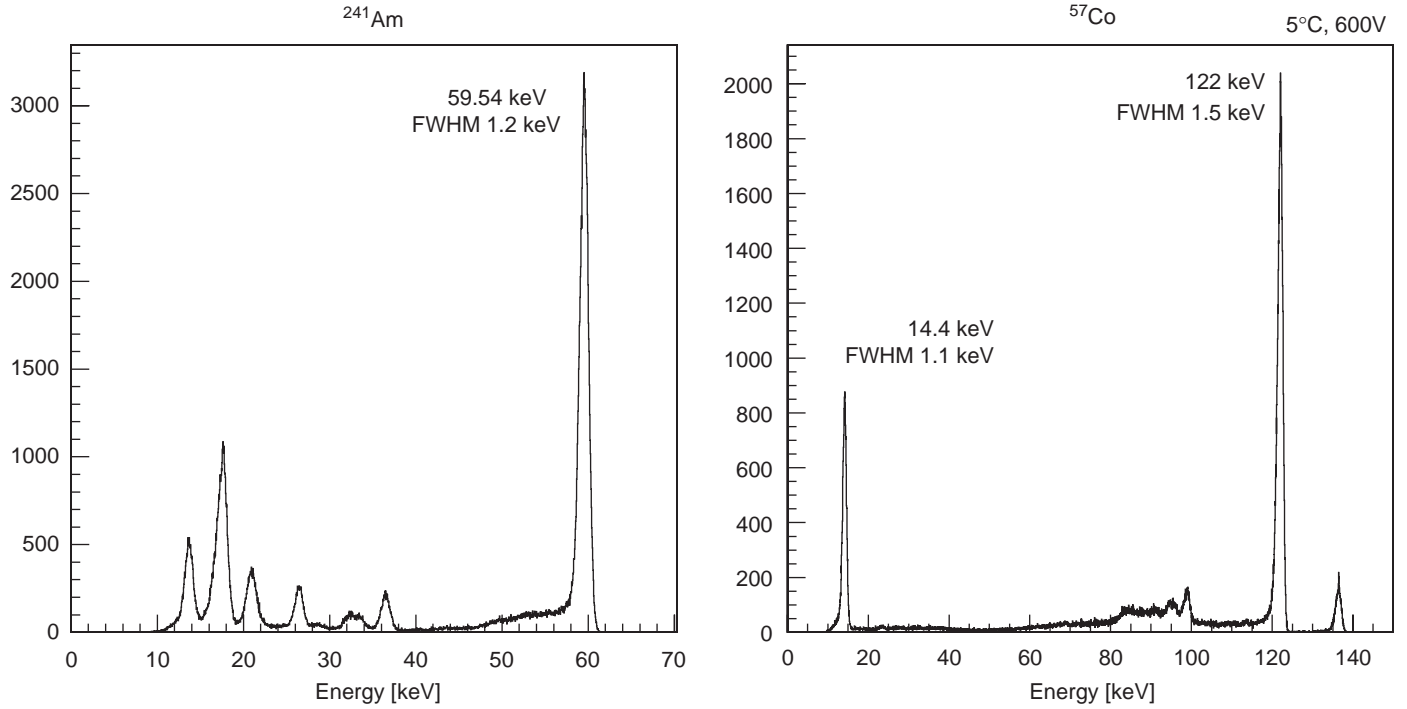


Fig. 7. The  $^{241}\text{Am}$  and  $^{57}\text{Co}$  spectra obtained from one of the CdTe pixel detector modules. These are summed spectra from all 64 pixels. The applied bias voltage is 600 V, and, the operating temperature is 5°C. The energy resolutions are 1.2 and 1.5 keV (FWHM) at 59.5 and 122 keV, respectively.

modules. For 64 spectra from all pixels, gain corrections were performed and then all corrected spectra were summed. The applied bias voltage was 600 V and the operating temperature was 5°C. The energy resolutions were 1.2 and 1.5 keV (FWHM) at 59.5 and 122 keV, respectively. The remarkably close resolution results were achieved for all the pixel modules, using the 74 CdTe devices selected from the leakage current measurement tests mentioned above.

## 5. CdTe stack detector as the absorber detector for the Compton camera

Stacking a number of thin CdTe detectors is a good way to obtain a high detection efficiency for higher energy gamma-rays. Since the carriers in CdTe have low mobility and a short life time, it is difficult for thick CdTe devices to accomplish full charge collections and high energy resolution. In our previous studies, we demonstrated that both good energy resolution and good detection efficiency can be achieved with the CdTe stack detector. These were achieved using planar CdTe diode detectors with a thickness of 0.5 mm [16–18]. As the absorber detector of the Compton camera, three-dimensional position detection capabilities are necessary in addition to good energy resolution and good detection efficiency. Therefore, in order to build a good absorber detector, we have constructed a CdTe pixel stack detector by stacking the CdTe pixel detector modules.

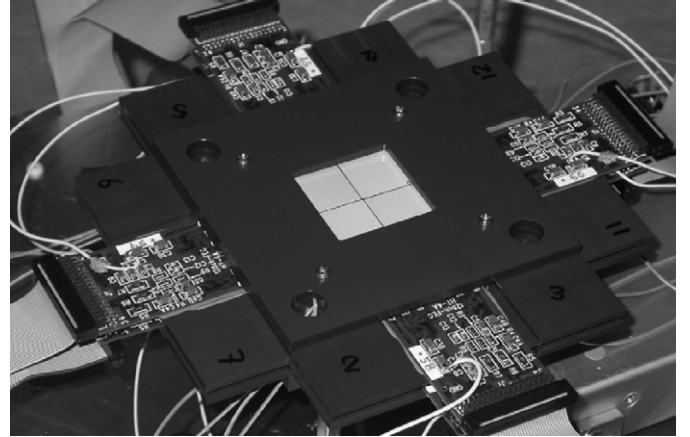


Fig. 8. The CdTe stack detector. Four layers are stacked. The stack pitch is 2 mm. A layer consists of  $2 \times 2 = 4$  CdTe pixel modules.

Fig. 8 shows the stack detector. It has four layers with each layer consisting of the  $2 \times 2 = 4$  pixel modules. A stack pitch between layers of 2 mm was attained in this detector.

In order to test performance as an absorber detector, we performed experiments using gamma-rays from radio isotopes. Fig. 9 shows obtained spectra of gamma-rays from  $^{133}\text{Ba}$ . Photo-electric absorption peaks are clearly seen in the spectra. The gray lines show the spectra from the first, the second, the third and the fourth layer, respectively. On the low energy side, only the first layer detects gamma-rays. On the other hand, the peak areas

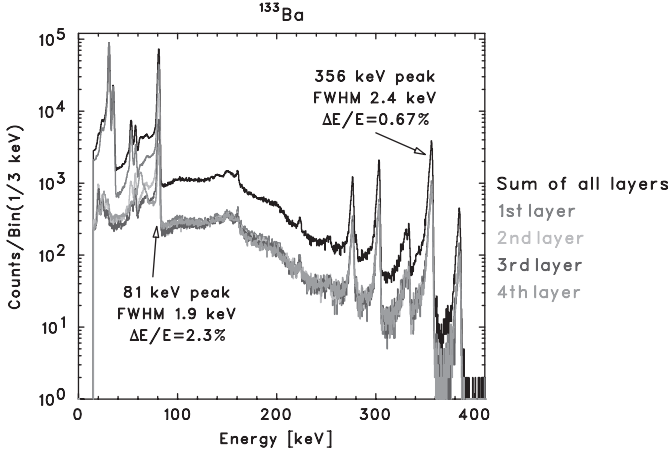


Fig. 9.  $^{133}\text{Ba}$  spectra obtained with the CdTe stack detector. The spectrum from each layer is shown in gray, and the summed spectrum of all layers is shown in black. The energy resolutions (FWHM) achieved are 1.9 and 2.4 keV at 81 and 356 keV, respectively.

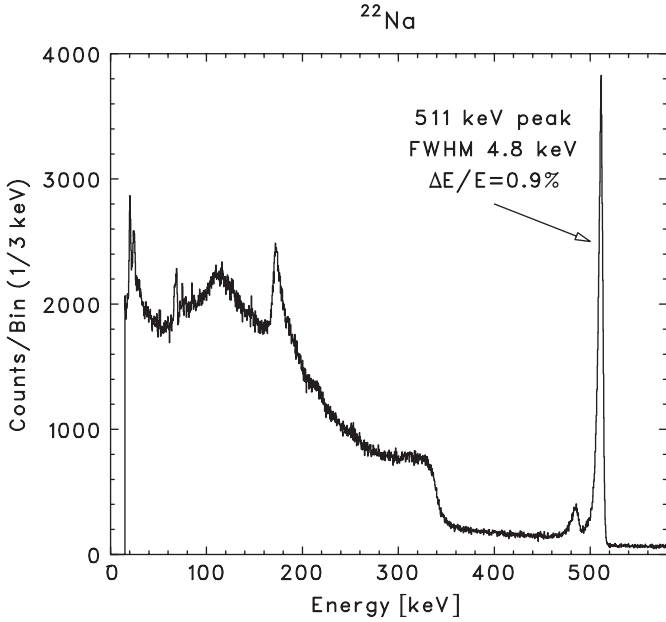


Fig. 10. A 511 keV gamma-ray spectrum obtained with the CdTe stack detector. A  $^{22}\text{Na}$  radioisotope is used. The FWHM for 511 keV gamma-ray peak is 4.8 keV ( $\Delta E/E \sim 0.9\%$ ).

detected in all layers are almost identical. This shows that the detection efficiency for higher energy gamma-rays was improved by stacking detectors. A 511 keV gamma-ray spectrum obtained with the CdTe stack detector is shown in Fig. 10. The achieved energy resolution is  $\Delta E(\text{FWHM})/E \sim 0.9\%$  at an operating temperature of  $-20^\circ\text{C}$  and under the bias voltage of 600 V.

## 6. Other applications of the CdTe pixel modules

Once CdTe pixel detector modules have been established, they have a variety of applications. One example is a

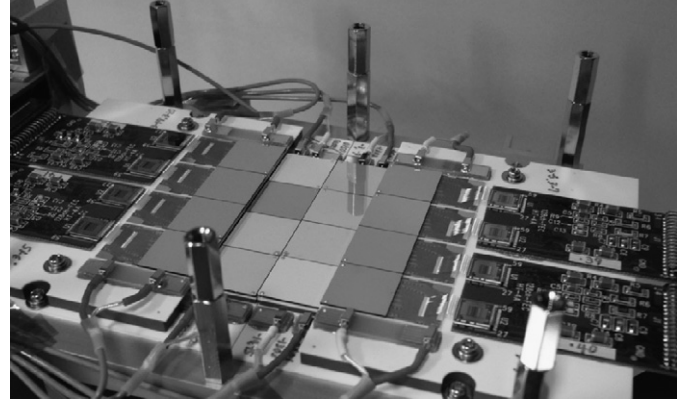


Fig. 11. The large area CdTe imager. The  $4 \times 4 = 16$  CdTe pixel modules are arranged in plates.

CdTe stack, as discussed in Section 5. This works as a gamma-ray probe with a high energy resolution.

Another application is as a large area CdTe imager. By arranging the modules, a CdTe imager with a large area and a high energy resolution can be created. Fig. 11 shows our constructed CdTe imager. The  $4 \times 4 = 16$  CdTe pixel detector modules are arranged on a plate. The total size of the imager is  $5.4\text{ cm} \times 5.4\text{ cm}$ . By attaching a collimator above the image, it works as a conventional gamma camera. Because the imager has a high energy resolution ( $\sim 1\%$ ), various gamma-ray lines can be easily separated in the obtained spectra. Therefore, the imager is capable of simultaneous multi tracer imaging in which different gamma-ray lines are used.

## 7. Conclusion

We have developed Si and CdTe imaging detectors for the Compton camera. The new four layer DSSD stack and the four layer CdTe pixel detector stack were, respectively, constructed as a scatterer detector and an absorber detector for the Compton camera. The noise performances of the stack detectors was found to be good. With the DSSD stack, we obtained an energy resolution of 1.5 keV (FWHM) for 60 keV gamma-ray photons. For the CdTe pixel detector stack, a  $\Delta E/E \sim 1\%$  energy resolution (FWHM) was achieved. As a next step, we will construct a new Si/CdTe Compton camera using the DSSD stack and the CdTe pixel detector stack.

## Acknowledgment

The authors would like to thank C. Baluta for reading the manuscript.

## References

- [1] T. Takahashi, et al., SPIE 4851 (2003) 1228.
- [2] T. Tanaka, et al., SPIE 5501 (2004) 229.
- [3] R. Ribberfors, Phys. Rev. B 12 (1975) 2067.

- [4] S. Watanabe, et al., IEEE Trans. Nucl. Sci. NS-52 (5) (2005) 2045.
- [5] T. Tanaka et al., Nucl. Instr. and Meth. A 568 (2006) 375.
- [6] T. Takahashi, et al., Nucl. Instr. and Meth. A 436 (2000) 111.
- [7] T. Takahashi, S. Watanabe, IEEE Trans. Nucl. Sci. NS-48 (4) (2001) 950.
- [8] T. Takahashi, et al., IEEE Trans. Nucl. Sci. NS-48 (3) (2001) 287.
- [9] T. Takahashi, et al., New Astron. Rev. 48 (2004) 309.
- [10] H. Odaka, et al., Nucl. Instr. and Meth. A (2007), doi:[10.1016/j.nima.2007.05.293](https://doi.org/10.1016/j.nima.2007.05.293).
- [11] S. Takeda, et al., Nucl. Instr. and Meth. A (2007), doi:[10.1016/j.nima.2007.05.305](https://doi.org/10.1016/j.nima.2007.05.305).
- [12] T. Tanaka, et al., New Astron. Rev. 48 (2004) 269.
- [13] T. Takahashi, et al., IEEE Trans. Nucl. Sci. NS-49 (2002) 1297.
- [14] K. Nakazawa, et al., IEEE Trans. Nucl. Sci. NS-51 (4) (2004) 1881.
- [15] S. Watanabe, et al., Nucl. Instr. and Meth. A 567 (2006) 150.
- [16] T. Takahashi, B. Paul, K. Hirose, C. Matsumoto, R. Ohno, T. Ozaki, K. Mori, Y. Tomita, Nucl. Instr. and Meth. A 436 (1999) 111.
- [17] S. Watanabe, et al., IEEE Trans. Nucl. Sci. NS-49 (3) (2002) 1292.
- [18] S. Watanabe, et al., Nucl. Instr. and Meth. A 505 (2003) 118.